Int. J. Electrochem. Sci., 13 **(2018)** 8960 – 8969, doi: 10.20964/2018.09.76

International Journal of ELECTROCHEMICAL SCIENCE
www.electrochemsci.org

Short Communication

Synthesis of a Crystal Violet-Cadmium Hydroxyquinoline Iodine Nanocomposite for the Photoelectrochemical Sensing of Ascorbic Acid

Shangwang Le[1], *Qian Jiang*[1], *Hongcheng Pan*[1,2,3,*]

[1] College of Chemistry and Bioengineering, Guilin University of Technology, 12 Jiangan Road, Guilin 541004, P. R. China.
[2] Guangxi College and University Key Laboratory of Food Safety and Detection, Guilin University of Technology, 12 Jiangan Road, Guilin 541004, P. R. China.
[3] Guangxi Key Laboratory of Electrochemistry and Magnetochemistry Functional Materials, Guilin University of Technology, 12 Jiangan Road, Guilin 541004, P. R. China.
[*]E-mail: hcpan@163.com

Received: 24 April 2018 / *Accepted:* 18 July 2018 / *Published:* 5 August 2018

A crystal violet-cadmium hydroxyquinoline iodine (CV-CdqI) nanocomposite was synthesized by adsorbing crystal violet (CV) onto cadmium hydroxyquinoline iodine (CdqI) nanowires. The CdqI nanowires were synthesized by mixing 100 mL of an aqueous 0.03 M CdI_2 solution with 100 mL of a 0.01 M 8-hydroxyquinoline ethanol solution in an ultrasonic bath. Scanning electron microscopy showed that CdqI exhibited a regular nanorod morphology with diameters of 30-60 nm and lengths of 400–600 nm. After adsorbing crystal violet, the CdqI nanowires become aggregated to form the CV-CdqI nanocomposite. X-ray powder diffraction (XRD) revealed that the XRD patterns of the CdqI nanowires and CV-CdqI nanocomposite are essentially the same, and no new phase was generated in the XRD pattern after the adsorption of CV. The fluorescence and photoelectrochemical (PEC) properties of the CV-CdqI nanocomposite were investigated. The CV-CdqI nanocomposite emits a yellow-green fluorescence with a maximum emission at 575 nm, which is similar to that of the CdqI nanowires. PEC measurements showed that the photocurrent response of the CV-CdqI nanocomposite spin-coated FTO electrode was stable and repeatable under the periodic on/off illumination of a 300 W xenon lamp at 0 V bias. Furthermore, the CV-CdqI/FTO electrode was used to construct a sensor for the PEC detection of ascorbic acid (AA). In the range of 1.4 to 10 μM, the photocurrent of the CV-CdqI/FTO electrode was inversely proportional to the concentration of AA with a detection limit of 0.2 μM. The method was used for the determination of AA in oranges (varied from 32.1 to 50.8 mg/100 g fresh weight).

Keywords: Crystal violet; cadmium hydroxyquinoline iodine; nanocomposite; photochemical sensing; ascorbic acid

1. INTRODUCTION

Metal-8-hydroxyquinoline (Mq_n) complexes and relevant nanostructures have been shown to be promising applications for (bio)sensing due to their excellent optical and electrochemical properties and their good abilities for interaction with a wide range of analytes[1-10]. Various Mq_n nanostructures have been fabricated, including Alq_3 (nanorods, nanowires, and nanoflowers) [4, 11, 12], Cdq_2 (nanorods, nanoribbons, and nanobelts) [7, 13, 14], Znq_2 (nanorods, nanoribbons, and octahedral particles) [15-17], Mnq_2 nanobelts [8], Cuq_2 nanoribbons [5], Gaq_3 nanorods [18], Niq_2 nanobelts [19], Coq_2 (nanobelts and nanosheets) [2, 19], Hgq_2 nanoribbons [20], and Erq_3 nanorods [21]. Recently, we reported a series of novel metal-hydroxyquinoline-halogen (MqX, M = Cd, Cu; X = Cl, Br, I) nanowires as novel sensing materials for fluorescence, electrochemiluminescence, and photoelectrochemistry (PEC) sensing [9, 10]. Among all these sensing methods, PEC combines the advantages of optical and electrochemical methods, making it a promising tool for analytical applications. Previously, we demonstrated that CdqI nanowires exhibit an excellent PEC property and show a good photoelectrochemical response for Cu^{2+} ions [9]. The photocurrent of CdqI nanowires, however, still needs to be improved for the analysis of real samples.

One possible strategy to further improve the photocurrent of CdqI nanowires is to form a nanocomposite structure, which contains two or more components. Such multicomponent nanocomposites have demonstrated enhanced photoelectric properties and been applied in various fields [22-30]. As we previously reported, some organic dyes (eosin Y and rhodamine B) can combine with Au nanoparticles to form nanocomposites, thereby increasing the PEC response to Hg^{2+} ions [29]. Inspired by this idea, we consider the combination of organic dyes and CdqI nanowires for tailoring and enhancing the PEC performance.

Crystal violet (CV) displays a characteristic absorption band in the visible region centered at approximately 605 nm and has been used as a photosensitizer in dye-sensitized solar cells (DSSCs). This sensitization of CV is produced by the dye's absorption of part of the visible light spectrum. Islam et al. studied the photocurrent growth and decay behavior of crystal violet dye-based solid-state PEC [31]. Additionally, Haldar et al. reported the photovoltaic property of crystal-violet dye-sensitized solid-state PEC [32]. In this work, we prepared a CV-CdqI nanocomposite and used it as a photoelectrode for enhanced PEC performance.

Ascorbic acid (AA) is an important cellular metabolite involved in many biochemical pathways. The detection of ascorbic acid has traditionally been achieved using high-performance liquid chromatography, absorption spectrophotometry, fluorescence, and electrochemical methods [33, 34]. As a newly emerged and promising sensing technique, PEC detection methods have received considerable research interest in bioanalysis. However, there have been only a few attempts in sensing AA using the PEC method. Compton et al. reported the photoelectrochemical determination of ascorbic acid by using methylene blue immobilized in α-zirconium phosphate [35]. Wang et al. synthesized flexible gold film electrodes for the photoelectrochemical sensing of ascorbic acid [36]. Kang et al. developed a double-channel photoelectrochemical method for the detection of ascorbic acid

using a g-C_3N_4/TiO_2 nanotubes hybrid film [37]. It is important to find new photoelectrode materials with a high photon-to-electricity conversion for the realization of the PEC sensing of AA. In this paper, we synthesize a CV-CdqI nanocomposite as a photoelectrode material for the development of a PEC sensor for the detection of AA.

2. EXPERIMENTAL

2.1. Chemicals and materials

Cadmium iodide (CdI_2), 8-hydroxyquinoline (Hq), and crystal violet were purchased from Aladdin Co. (Shanghai, China). Anhydrous alcohol, dimethylsulfoxide (DMSO), acetic acid (HAc), and acetone were purchased from Xilong Chemical Lit. Co. (Shantou, China). Fluorine-doped tin oxide (FTO) glass electrodes (13×30×1.1 mm) were from Kaivo Optoelectronic (Zhuhai, China). Other reagents were of analytical grade. Ultrapure water (resistivity > 18 MΩ·cm) was obtained from a Milli-Q purification system (Millipore, USA) and was used in all experiments.

2.2. Preparation of the CV-CdqI nanocomposite

The CdqI nanowires were synthesized via a sonochemical-assisted method, according to our published procedure [9]. The typical synthesis procedure was as follows: 100 mL of an aqueous 0.03 M CdI_2 solution was mixed with 100 mL of a 0.01 M 8-Hq ethanol solution. The mixture was placed into an ultrasonic bath at 50 ℃ for 2 h. The nanorods were purified using five 20-min-long centrifugation cycles at 4000 revolutions per minute (RPM). At the end of each centrifugation cycle, the supernatant was removed, and the precipitate was redispersed in ethanol solution, followed by the addition of 35 mL of a 0.01 M crystal violet solution and thorough mixing. The mixture was placed into an ultrasonic bath at 50 °C for 2 h. Subsequently, the solution was allowed to cool down to room temperature. The precipitate was then collected by centrifugation at 4000 RPM for 10 min, washed 3 times with an ethanol solution (50%, *v*/*v*), and air dried at 40 °C for 4 h.

2.3. Characterization and measurements

Scanning electron microscopy (SEM) imaging was performed on a Hitachi S-4800 scanning electron microscope (Hitachi, Tokyo, Japan). X-ray powder diffraction (XRD) measurements were performed on an X'Pert PRO X-ray diffractometer (Philips, Eindhoven, Netherlands). Infrared spectra were measured by Fourier transform infrared spectroscopy (FTIR, Nicolet iS10, Thermo Fisher Scientific, USA). Fluorescence spectra were gathered using a fluorescence spectrophotometer (CaryEclipse, VARIAN, USA). The electrochemiluminescence (ECL) measurements were performed on an MPI-E ECL analysis system (Xi'an Remex, Xi'an, China). Photoelectrochemical measurements were made using a homemade photoelectrochemical system. A 300-W xenon lamp was used as the irradiation source. The photocurrent was measured on a CHI 660B electrochemical workstation

(Chenhua, Shanghai, China). Prior to the measurement, the sample was spin-coated on a fluorine-doped tin oxide (FTO) glass substrate and employed as the working electrode. A Pt wire was used as the counter electrode, and a saturated Ag/AgCl electrode was used as the reference electrode. All photocurrent measurements were performed at a constant potential of 0 V (*vs* saturated Ag/AgCl) in a solution of 0.2 M acetic acid buffer (pH = 5) and 0.1 M KNO_3.

2.4. Preparation of real samples

Oranges was bought from a supermarket in Guilin, China. The pericarps of the oranges were removed, and then the fruits (3 g) were homogenized with 20 mL of 2% (v/v) HAc by using a mortar. The extracts were centrifuged at 4000 revolutions per minute for 30 min. After centrifugation, the supernatant was transferred into a 200-mL volumetric flask and diluted with 2% (v/v) HAc. Measurements of the samples (0.8 mL) were carried out immediately after preparation steps.

3. RESULTS AND DISCUSSION

3.1. SEM and XRD of the CdqI nanowires and CV-CdqI nanocomposite

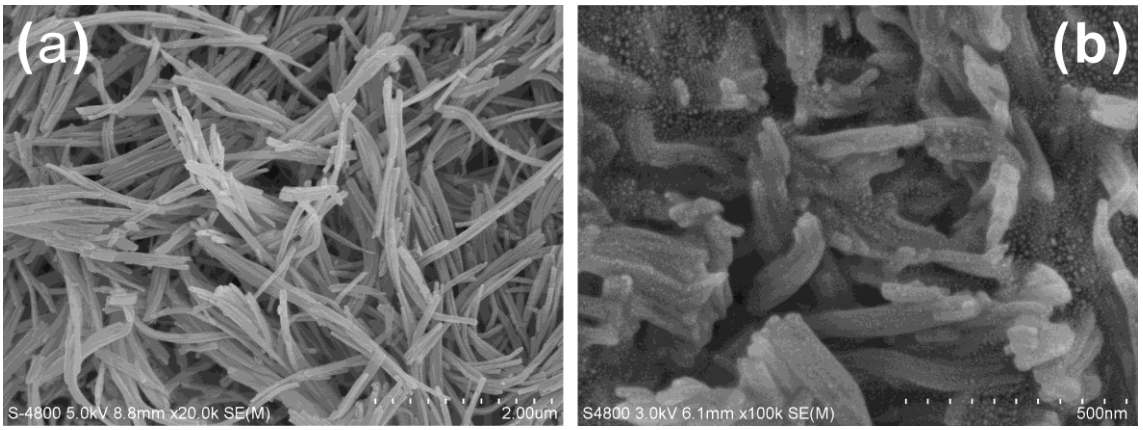

Figure 1. SEM images of the (a) CdqI nanowires and (b) CV-CdqI nanocomposite.

The surface morphology of CdqI nanowires and the CV-CdqI nanocomposite was determined by SEM. The CdqI nanowires have a diameter of approximately 30–60 nm and a length of approximately 400–600 nm (Figure 1a). No adsorbents were observed on the surface of the CdqI nanowires. As shown in Figure 1b, the surface morphology of the CV-CdqI nanocomposite was conspicuously different from that of the CdqI nanowires. Although the nanowire structure of CdqI in the CV-CdqI nanocomposite remained relatively unchanged, we observed an amorphous material adsorbed onto a substantial part of the CdqI nanowire surface. We infer that the adsorbed material most likely consists of CV molecules. Figure 2 depicts that the XRD patterns of the CdqI nanowires and CV-CdqI nanocomposite are essentially the same, and no new phase is generated in the XRD patterns after the adsorption of CV. These results suggest that no change occurs in the crystal structure of CdqI nanowires, and CV is present in an amorphous form.

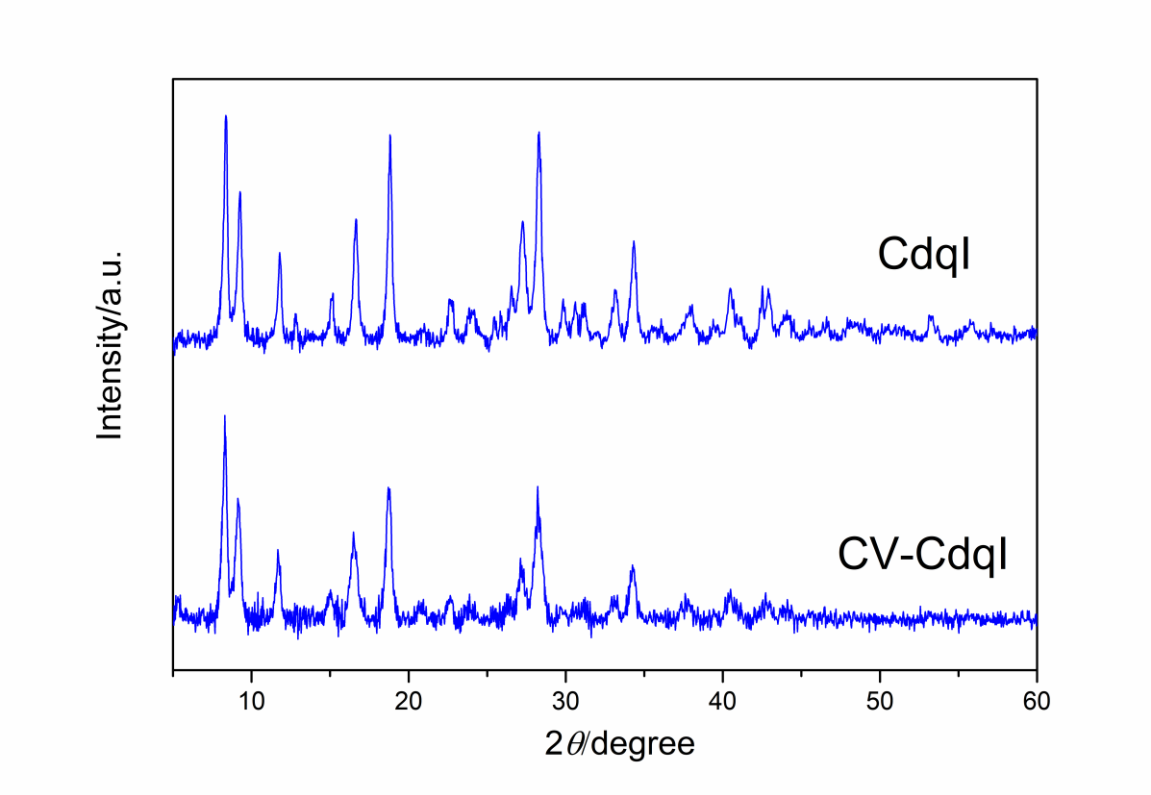

Figure 2. XRD of the (a) CdqI nanowires and (b) CV-CdqI nanocomposite.

3.2. UV-vis spectra of the CV-CdqI nanocomposite

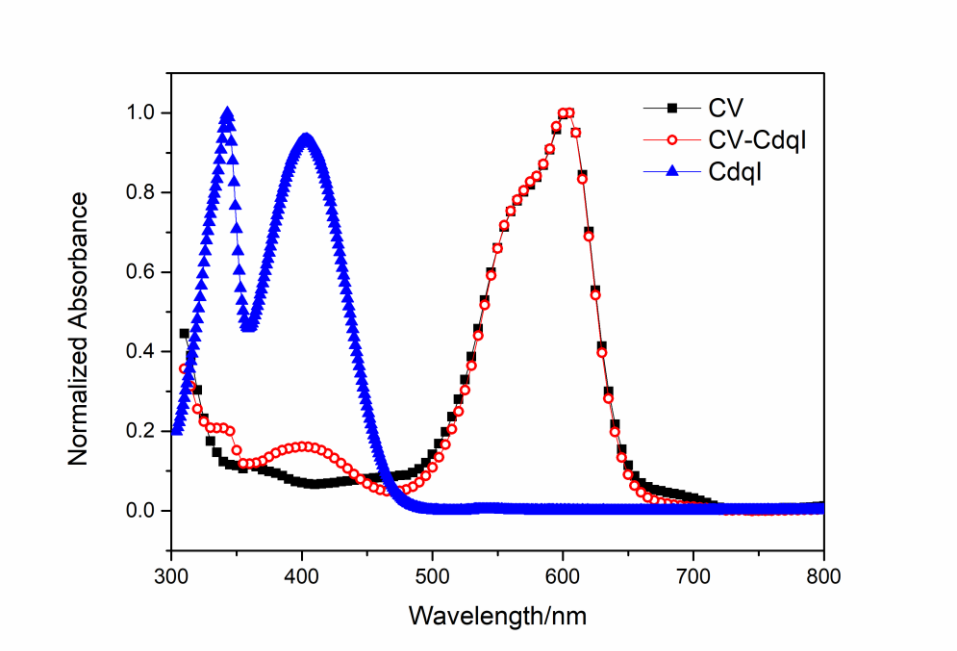

Figure 3. UV-vis spectra of the (a) CV, (b) CdqI nanowires, and (b) CV-CdqI nanocomposite in DMSO solutions.

We compared the UV-vis spectra of CV, CdqI nanowires and the CV-CdqI nanocomposite (Figure 3). CV displayed a wide and strong absorption peak at 605 nm. The CdqI nanowires exhibited two peaks at 402 and 343 nm. The UV-vis spectrum of the CV-CdqI nanocomposite looks similar to the addition of the spectra of CV and the CdqI nanowires. A wide and strong absorption peak at 605 nm was observed in the spectrum of The CV-CdqI nanocomposite. We attribute this peak to the molecular absorption of CV. The maximum absorption wavelength of CV in the CV-CdqI nanocomposite did not shift compared to that of the CV solution. Two characteristic peaks of the CdqI nanowires at 402 and 340 nm were observed in the CV-CdqI nanocomposite. These results indicate that no chemical reactions occur during the formation of the CV-CdqI nanocomposite. On the basis of the above observations, we infer that the formation of the CV-CdqI nanocomposite is mainly driven by several noncovalent interactions, such as hydrogen bonding, π···π stacking, electrostatics and hydrophobic interactions.

3.3. Fluorescence spectra and PEC of the CdqI nanowires and CV-CdqI nanocomposite

To investigate the fluorescence property of the CV-CdqI nanocomposite, the sample was dispersed in DMSO and excited at 350 nm, while the emission was collected by a fluorescence spectrophotometer. The fluorescence of the CdqI nanowires was also studied for comparison. The DMSO solution of the CdqI nanowires emits a yellow-green fluorescence with a maximum emission at 575 nm. Similarly, the DMSO solution of the CV-CdqI nanocomposite produces fluorescence at the same wavelength. These results, combined with the XRD and UV-vis spectra, support our assumption that the formation of the CV-CdqI nanocomposite does not change the structure of CdqI.

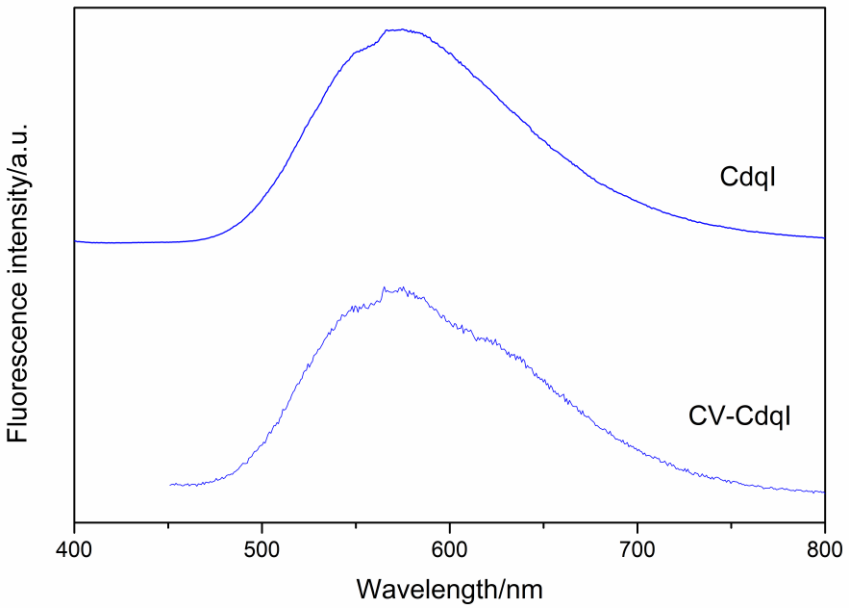

Figure 4. Fluorescence spectra of the CdqI nanowires and CV-CdqI nanocomposite in DMSO solutions. The excitation wavelength is 350 nm.

We further studied the photoelectrochemistry of the CV-CdqI nanocomposite. PEC experiments were performed using a fluorine-doped tin oxide (FTO) electrode spin-coated with CV-CdqI nanocomposite films at a fixed bias of 0 V versus Ag/AgCl with on–off illumination cycles of a 300-W xenon lamp. It was found that the photocurrent response for the CV-CdqI nanocomposite was stable and repeatable over many light/dark cycles (Figure 5). A very low current indicates that no chemical or electrochemical reaction of electrolysis occurred at the applied bias of 0 V under dark conditions. According to Figure 5, the CV-CdqI nanocomposite exhibited a quick response to light switching. This rapid response is most likely related to the facilitated exciton migration and carrier transportation in the CV-CdqI nanocomposite. For comparison, the CdqI nanowires were spin-coated onto an FTO electrode, and the photocurrent was measured under the same experimental conditions. Although the CdqI/FTO photoelectrode exhibited a quick response to light switching, the photocurrent is much smaller than that of the CV-CdqI/FTO photoelectrode. The photocurrent of the CV-CdqI/FTO photoelectrode was enhanced up to 3.4-fold compared to that of the CdqI/FTO photoelectrode. Such an enhanced PEC property may have promising applications in photoelectrochemical sensors.

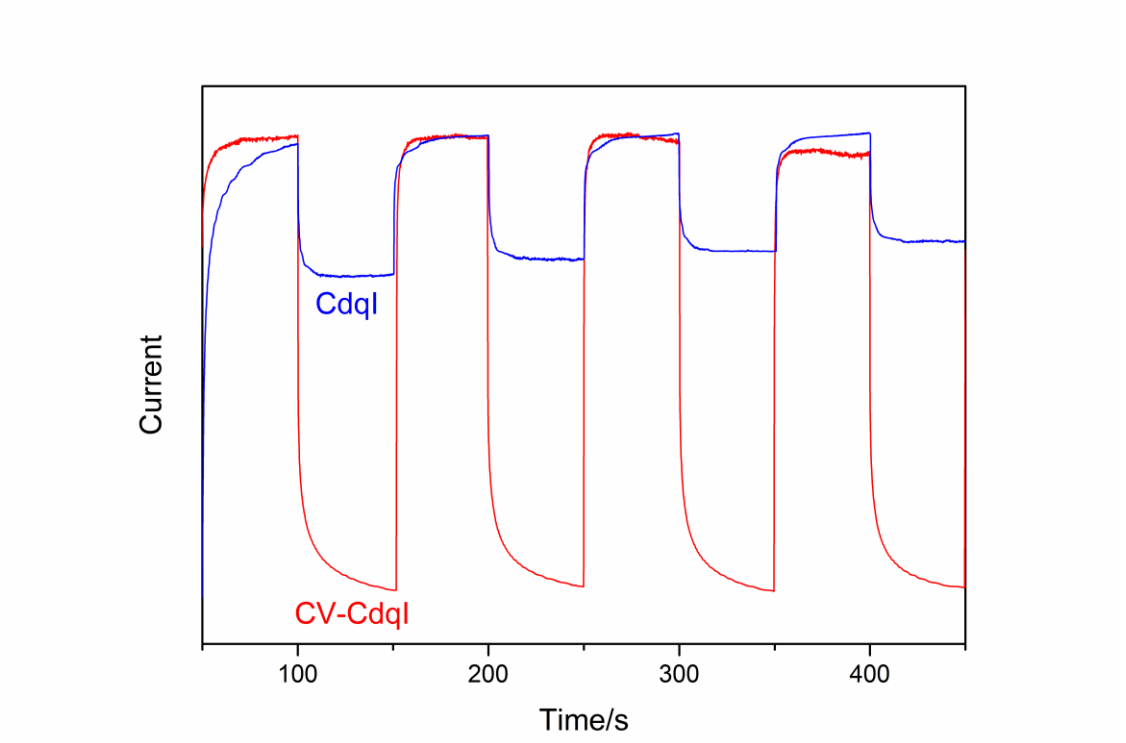

Figure 5. Photocurrent–time curves of the CdqI nanowires/FTO and CV-CdqI nanocomposite/FTO electrodes at a bias of 0 V versus Ag/AgCl with on–off illumination cycles of a 300-W xenon lamp.

3.4. PEC sensing of AA using the CV-CdqI nanocomposite

We investigated the potential applications of the CV-CdqI nanocomposite in PEC sensing. The CV-CdqI/FTO electrode were employed to develop a PEC method for detecting AA. Figure 6 depicts the photocurrent-time response of the CV-CdqI/FTO electrode arising from the successive addition

(1.4 μM increments) of AA to a NaAc-HAc solution (0.2 M, pH 5.0). It is evident that the subsequent additions of AA resulted in a photocurrent decrement. The analysis of the photocurrent as a function of the AA concentration is depicted in the inset of Figure 6, which reveals a linear response over the range of 1.4 to 10 μM, and a detection limit of 0.2 μM was measured. Compared with previous reports, this detection limit is lower than or comparable to those obtained by photoelectrochemical methods [35, 36, 38-41]. Common interferents including uric acid, malic acid, citric acid, fructose, glucose, Na^+, K^+, Ca^{2+}, and Mg^{2+} did not significantly interfere with the detection of AA. Using the CV-CdqI/FTO electrodes, we detected AA in the real orange samples. The results were satisfactory, with the recoveries ranging from 95.7% to 99.3%, as listed in Table 1.

Table 1. Results of AA determination in the real orange samples.

Orange sample	Added (mg/100 g)	Found (mg/100 g)	Recovery (%)
1#	-	32.1	-
	30	61.9	99.3
2#	-	50.8	-
	30	79.5	95.7

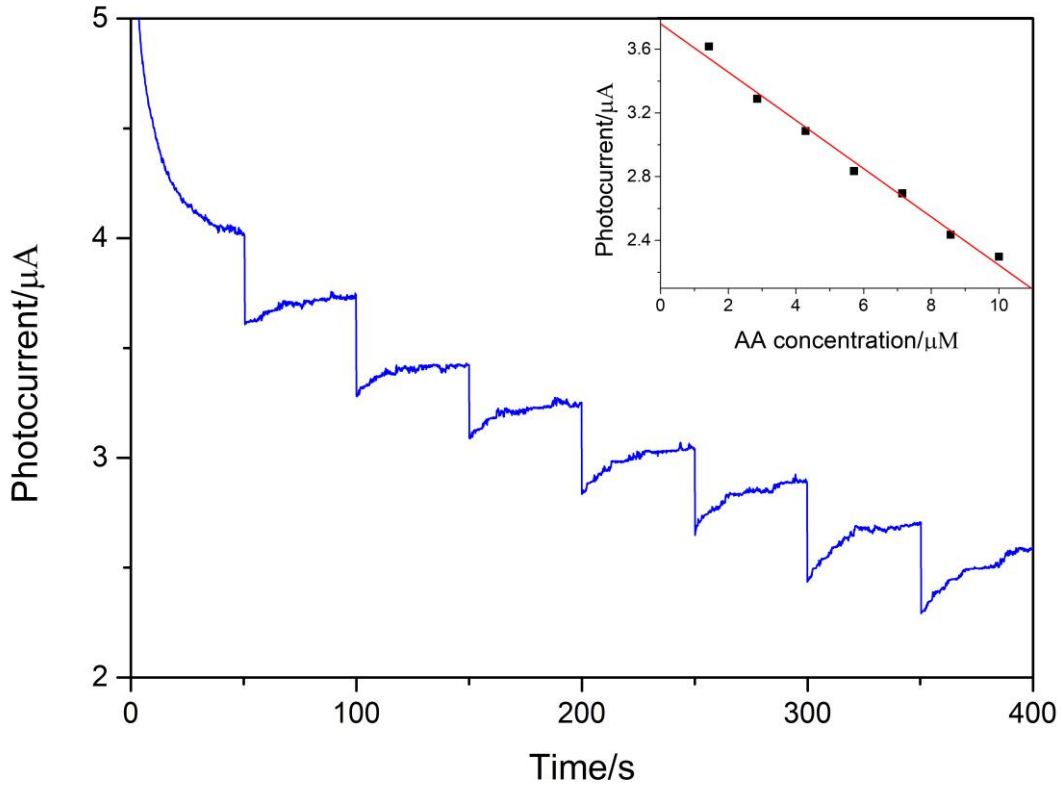

Figure 6. Photocurrent–time curves of successive additions of 1.4 μM AA at the CV-CdqI/FTO electrode in a solution containing 13 mL of NaAc-HAc buffer (0.2 M, pH 5.0) and 1 mL of 0.1 M KNO_3. Upper-right inset: calibration plot of photocurrent versus AA concentration.

Although the details of the mechanism of the PEC sensing of AA are still not fully understood, the CV-CdqI nanocomposite, CV, and AA may play different roles in the whole PEC process. The CV-CdqI nanocomposite is the main material for the photogenerated electron-hole pairs. CV can serve as a sensitizer for photoexcitation of the CV-CdqI nanocomposite. According to previous reports, AA can react with some organic dyes, such as methylene blue and toluidine blue [39]. From this we infer that AA reacts with CV, resulting in the desensitization of CV and the decrease in the photocurrent.

4. CONCLUSIONS

We synthesized a CV-CdqI nanocomposite and investigated its structure, composition, and properties. The evidence from this study suggests that no change occurs in the crystal structure of the CdqI nanowires and the presence of an amorphous form of CV. We infer that the formation of the CV-CdqI nanocomposite is mainly driven by the noncovalent interactions. The CV-CdqI nanocomposite exhibited excellent fluorescence and PEC properties. We used CV-CdqI nanocomposite-coated FTO as a photoelectrode to construct a sensor for the PEC detection of AA. The photocurrent of the CV-CdqI/FTO electrode declined with subsequent additions of AA. The sensor presented a linear response range from 1.4 to 10 μM of AA with a detection limit of 0.2 μM. Such PEC sensors provide great promise for future practical applications.

ACKNOWLEDGEMENTS
This work was supported by the National Natural Science Foundation of China (21265005), the Guangxi Natural Science Foundation (2017GXNSFAA198340), the project of the high-level innovation team and outstanding scholars in the Guangxi colleges and universities, the Guangxi College and University Key Laboratory of Food Safety and Detection, the Collaborative Innovation Center for Water Pollution Control and Water Safety in the Karst area, and the Guangxi Key Laboratory of Environmental Pollution Control Theory and Technology.

References

1. L.M.A. Monzon, F. Burke and J.M.D. Coey, *J. Phys. Chem. C*, 115 (2011) 9182.
2. H. Li and Y. Li, *Nanoscale*, 1 (2009) 128.
3. H. Bi, H. Zhang, Y. Zhang, H. Gao, Z. Su and Y. Wang, *Adv. Mater.*, 22 (2010) 1631.
4. C.-J. Mao, D.-C. Wang, H.-C. Pan and J.-J. Zhu, *Ultrason. Sonochem.*, 18 (2011) 473.
5. Q. Shao, T. Wang, X. Wang and Y. Chen, *Front. optoelectron. China*, 4 (2011) 195.
6. Z. Yin, B. Wang, G. Chen and M. Zhan, *J. Mater. Sci.*, 46 (2011) 2397.
7. X.-B. Chen, Z. Gong, B.-C. Zhou, X.-W. Hu, C.-J. Mao, J.-M. Song, H.-L. Niu and S.-Y. Zhang, *Mater. Lett.*, 75 (2012) 155.
8. X.-D. Yang, X.-B. Chen, C.-J. Mao, J.-M. Song, H.-L. Niu and S.-Y. Zhang, *J. Alloys Compd.*, 590 (2014) 465.
9. S. Huang, G. Pang, X. Li, J. Li and H. Pan, *J. Nanopart. Res.*, 19 (2017) 392.
10. H. Pan, H. Lin, Q. Shen and J.-J. Zhu, *Adv. Funct. Mater.*, 18 (2008) 3692.
11. J. S. Hu, H. X. Ji, A. M. Cao, Z. X. Huang, Y. Zhang, L. J. Wan, A. D. Xia, D. P. Yu, X. M. Meng and S. T. Lee, *Chem. Commun.*, (2007) 3083.

12. Y.S. Zhao, C. Di, W. Yang, G. Yu, Y. Liu and J. Yao, *Adv. Funct. Mater.*, 16 (2006) 1985.
13. W. Chen, Q. Peng and Y. Li, *Cryst. Growth Des.*, 8 (2008) 564.
14. X. Wang, M. Shao and L. Liu, *J. Mater. Sci.: Mater. Electron.*, 22 (2010) 120.
15. H. Pan, F. Liang, C.-J. Mao, J.-J. Zhu and H.-Y. Chen, *J. Phys. Chem. B*, 111 (2007) 5767.
16. X.-B. Chen, X.-D. Yang, X.-W. Hu, C.-J. Mao, J.-M. Song, H.-L. Niu and S.-Y. Zhang, *Mater. Res. Bull.*, 48 (2013) 1675.
17. X. Wang, M. Shao and L. Liu, *Synth. Met.*, 160 (2010) 718.
18. F.F. Muhammad and K. Sulaiman, *Mater. Chem. Phys.*, 148 (2014) 473.
19. L. Liu, L. Wang and D. Jia, *J. Coord. Chem.*, 61 (2008) 1019.
20. L. Liu, M. Shao and X. Wang, *Front. optoelectron. China*, 3 (2010) 228.
21. S. Dang, Q. Liu, K. Liu, Z. Guo, L. Sun, S. Song and H. Zhang, *Cryst. Growth Des.*, 10 (2010) 4662
22. R. Liu, *Materials*, 7 (2014) 2747.
23. Q. Li, X. Li, S. Wageh, A.A. Al-Ghamdi and J. Yu, *Adv. Energy Mater.*, 5 (2015) 1500010.
24. Y.V. Kaneti, J. Tang, R.R. Salunkhe, X. Jiang, A. Yu, K. C. W. Wu and Y. Yamauchi, *Adv. Mater.*, 29 (2017) 1604898.
25. J. Xu, Y. Wang and S. Hu, *Microchim. Acta*, 184 (2017) 1.
26. J. Munoz and M. Baeza, *Electroanal.*, 29 (2017) 1660.
27. A. Kaushik, R. Kumar, S.K. Arya, M. Nair, B.D. Malhotra and S. Bhansali, *Chem. Rev.*, 115 (2015) 4571.
28. W. Zhu, X. Li, W. Liu, Z. Chen, J. Li and H. Pan, *Int. J. Electrochem. Sci.*, 12 (2017) 4970.
29. Y. Yuan, G. Pang, X. Li, W. Zhu and H. Pan, *Anal. Methods*, 9 (2017) 5586.
30. H. Tang, J. Zheng, J. Li, Q. Xu and H. Pan, *Optoelectron. Adv. Mat.*, 11 (2017) 671.
31. M. R. Islam, S. Maity, A. Haldar, N. B. Manik and A. N. Basu, *Ionics*, 18 (2011) 209.
32. A. Haldar, S. Maity and N. B. Manik, *Ionics*, 14 (2008) 427.
33. L. Xing and Z. Ma, *Prog. Chem.*, 28 (2016) 1705.
34. Y. Matsuoka, M. Yamato and K.-I. Yamada, *J. Clin. Biochem. Nutr.*, 58 (2016) 16.
35. J.A. Cooper, K. E. Woodhouse, A.M. Chippindale and R.G. Compton, *Electroanalysis*, 11 (1999) 1259.
36. J. Wang, J. Sun, C. Hu, Z. Liu and S. Hu, *J. Electroanal. Chem.*, 759 (2015) 2.
37. Q. Kang, X. Wang, X. Ma, L. Kong, P. Zhang and D. Shen, *Sensor. Actuat. B-Chem.*, 230 (2016) 231.
38. H. Li, Q. Gao, L. Chen and W. Hao, *Sensor. Actuat. B-Chem.*, 173 (2012) 540.
39. Y. Dilgin, Z. Dursun, G. Nisli and L. Gorton, *Anal. Chim. Acta*, 542 (2005) 162.
40. J.A. Cooper, M. Wu and R.G. Compton, *Anal. Chem.*, 70 (1998) 2922.
41. R.M. Mazhabi, L. Ge, H. Jiang and X. Wang, *Biosens. Bioelectron.*, 107 (2018) 54.